

Semi Microscopic Description of ^{84}Kr

H. Dias

Instituto de Física da Universidade de São Paulo, Brasil

F. Krmpotić*

Departamento de Física, Facultad de Ciencias Exactas,
Universidad Nacional de la Plata, Argentina
and Instituto de Física da Universidade de São Paulo, São Paulo, Brasil

L. Losano**

Instituto de Física da Universidade de São Paulo, Brasil

R.C. Mastroleo***

Divisão de Física Teórica, Instituto de Estudos Avançados,
Centro Técnico Aeroespacial, São José dos Campos, Brasil

Received May 6, 1985; revised version February 5, 1986

The experimental information on the ^{84}Kr nuclei is compared with the model calculation in which two neutron holes are coupled to the vibrational field. Based on the lower-order terms of a perturbative expansion of the $E2$ and $M1$ transition matrix elements, a simple rule is obtained for the sign and the magnitude of the $\delta(E2/M1)$ ratios for the transitions between the second and first 2^+ states in some vibrational nuclei.

[Nuclear structure ^{84}Kr , calculated levels J , π and $\delta(E2/M1)$, Cluster-phonon model. Pairing interaction].

PACS: 21.60.Gx; 23.20.Gq; 21.10.Hw

I. Introduction

The directional correlations of coincident γ transitions have recently been measured for several cascades in the ^{84}Kr nucleus [1]. Besides establishing spins of a number of levels, this measurement also gives information on the multipole mixing ratios $\delta(E2/M1)$, which is of considerable importance in

providing a better understanding of the structure of this nucleus.

More specifically, while the spins and parities of the low-lying states of ^{84}Kr indicate a collective quadrupole vibrational structure, the predominance of $M1$ in the multipolarity of several gamma transitions strongly suggests that also the single-particle degrees of freedom play an important role.

In view of the above-mentioned properties we propose in the present work a theoretical interpretation of the structure of ^{84}Kr nucleus, and in particular of the ratios $\delta(E2/M1)$ measured in Ref. 1, within the two-hole cluster-quadrupole vibration coupling model.

* Member of the Carrera del Investigador Científico, Consejo Nacional de Investigaciones Científicas y Técnicas, Argentina

** Permanent Address: Departamento de Física da Universidade Federal da Paraíba, João Pessoa, Paraíba, Brasil

*** Present Address: Department of Physics, University of Texas, Austin, TX 78712, USA

II. The Nuclear Model and Parameters

A detailed description of the model is given in Refs. 2 and 3. Here we only sketch the main formulas in order to establish the notation. The system is described by the Hamiltonian

$$H = H_0 + H_{\text{res}} + H_{\text{int}} \quad (1)$$

where H_0 is the energy of the unperturbed system represented by a quadrupole vibrational field and by two valence neutrons in a central field. The residual interaction energy among the neutrons in the shell-model cluster, H_{res} , only includes explicitly the pairing force. The particle-vibration interaction is given by the expression

$$H_{\text{int}} = -\frac{\beta_2}{\sqrt{5}} \sum_{\mu} [b_2^{\mu+} + (-)^{\mu} b_2^{-\mu}] \sum_{i=1}^2 k(r_i) Y_{2\mu}^*(\theta_i, \phi_i) \quad (2)$$

where $k(r_i)$ is the interaction intensity and β_2 is the quadrupole deformation parameter.

The eigenvalue problem is solved in the basis $[[j_1 j_2] J, NR] I\rangle$, where $j=(nlj)$ stands for the quantum numbers of the hole states, J is the total angular momentum of the two holes, N and R represent the phonon number and the angular momentum, respectively, and I is the total angular momentum.

The matrix element of H_{int} are parametrized by the coupling constant a defined as

$$a = \frac{\langle k \rangle \beta_2}{\sqrt{20\pi}} \quad (3)$$

where $\langle k \rangle$ is the mean value of the radial matrix element of the interaction.

The electric quadrupole and magnetic-dipole operators consist of a particle and a collective part

$$\begin{aligned} \mathcal{M}(E2, \mu) &= e_p^{\text{eff}} \sum_{i=1}^2 r_i^2 Y_{2\mu}(\theta_i, \phi_i) \\ &+ \frac{3R_0^2}{4\pi} e_v^{\text{eff}} [b_2^{\mu+} + (-)^{\mu} b_2^{-\mu}], \end{aligned} \quad (4)$$

$$\mathcal{M}(M1, \mu) = \left(\frac{3}{4\pi}\right)^{1/2} [g_R R_{\mu} + g_l L_{\mu} + g_s S_{\mu}] \mu_N, \quad (5)$$

where e_p^{eff} is the effective particle charge, $e_v^{\text{eff}} = Ze\beta_2/\sqrt{5}$ is the effective vibrator charge, and g_R , g_l and g_s are, respectively, the collective, orbital and spin gyromagnetic ratios.

The mixing ratio $\delta(E2/M1)$ for the $E2$ and $M1$ transitions reads [4]

$$\delta(E2/M1) = 0.835(E_{\gamma}/\text{MeV})(\mathcal{D}/eb\mu_N^{-1}) \quad (6)$$

with

$$\mathcal{D} = \frac{\langle I_i \| \mathcal{M}(E2) \| I_f \rangle}{\langle I_i \| \mathcal{M}(M1) \| I_f \rangle}. \quad (7)$$

The matrix elements of the $E2$ and $M1$ operators are expressed in the forms

$$\langle I_i \| \mathcal{M}(E2) \| I_f \rangle = (e_p^{\text{eff}} A + e_v^{\text{eff}} B) e b, \quad (8a)$$

$$\langle I_i \| \mathcal{M}(M1) \| I_f \rangle = (g_s C + g_l D + g_R E) \mu_N \quad (8b)$$

and the quantities A , B , C , D and E are calculated from the model wave functions.

The Hamiltonian was diagonalized with the following set of parameters:

(a) pairing strength $G = 0.29$ MeV, which follows from the estimate of Kisslinger and Sorensen [5] ($G = 25/A$ MeV);

(b) phonon energy $\hbar\omega_2 = 1.56$ MeV, is the experimental energy of 2_1^+ state in the single-closed-shell ^{86}Kr nucleus [6];

(c) particle-vibration coupling constant $a = 0.74$ MeV, which results from $\beta_2 = 0.13$ (as measured in the Coulomb excitation process on ^{86}Kr (Ref. 6)) and $\langle k \rangle \simeq 45$ MeV (as estimated numerically using wave functions obtained from the Woods-Saxon potential [7]);

(d) single particle energies $\varepsilon_{g_{9/2}} = 0$, $\varepsilon_{p_{1/2}} = 0.80$ MeV, $\varepsilon_{p_{3/2}} = 1.35$ MeV and $\varepsilon_{f_{5/2}} = 1.8$ MeV, were taken from the work of Boer et al. [8].

In this parametrization, without an adjustable parameter, we diagonalize the Hamiltonian by including all the vibrational states up to three phonons.

The electromagnetic properties were evaluated with the usual values of the effective electric charge and effective gyromagnetic ratios.

$$e_p^{\text{eff}} = 0.5e, \quad e_v^{\text{eff}} = \frac{\beta_2 Z e}{\sqrt{5}} = 2.09,$$

$$g_R = Z/A = 0.43, \quad g_l = 0,$$

$$g_s^{\text{eff}} = 0.6g_s^{\text{free}} = -2.30.$$

III. Results and Discussion

In order to test the parametrization quoted in the previous section we first briefly discuss the available experimental data for the $N = 49$ nuclei [9–12]. The energy spectra are compared in Fig. 1 and the results for the electric quadrupole and magnetic dipole moments of the ground state are shown in Table 1. It should be noted that the agreement between the calculated and the measured energy spectra for ^{85}Kr , ^{87}Sr , ^{89}Zr and ^{91}Mo nuclei can be improved

Table 1. Comparison of experimental and theoretical electric quadrupole and magnetic dipole moments for the ground state ($I^\pi = 9/2^+$) in $N=49$ nuclei

	Experiment		Theory
	^{85}Kr	^{87}Sr	
$Q(eb)$	0.43 ^a	0.335 ± 0.020^b	0.37
$\mu(\mu_N)$	1.005 ^a	1.0924 ± 0.0007^b	1.06

^a Ref. 10;^b Ref. 9

by lowering the particle-phonon coupling constant. As an example, in Fig. 1 is also exhibited the calculated spectrum for $a=0.5$ MeV.

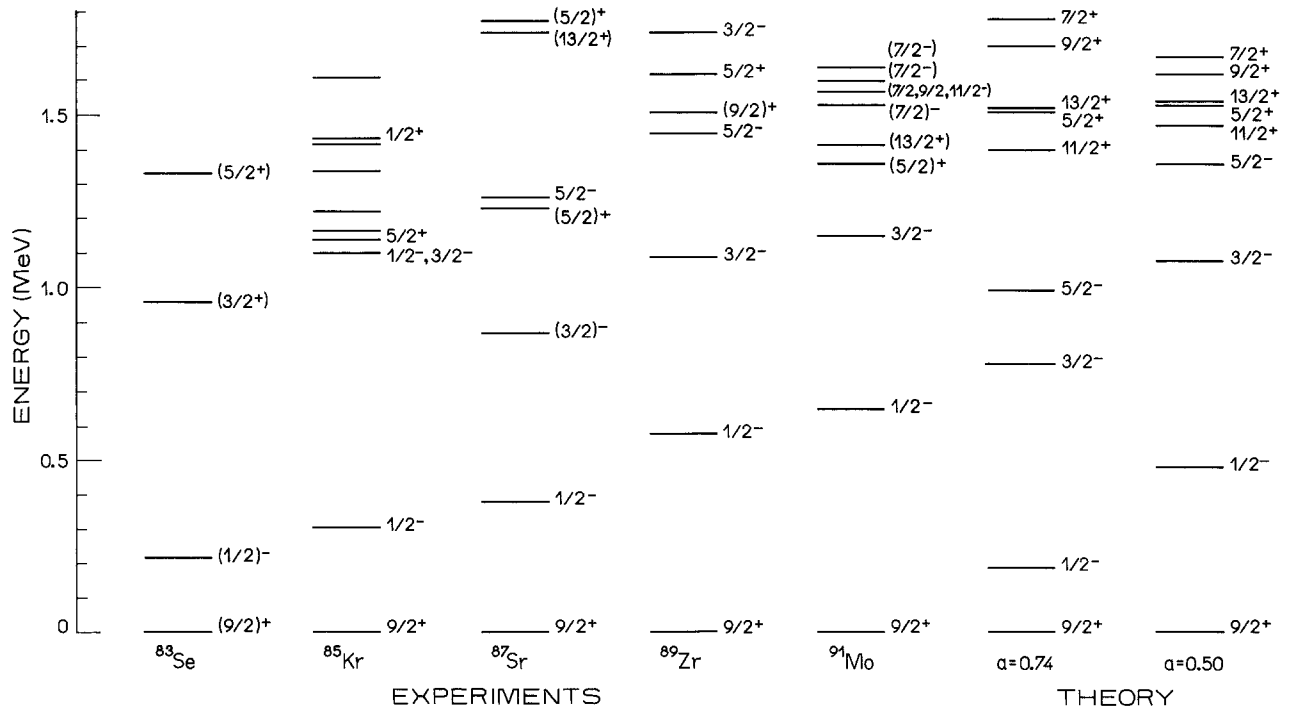
The calculated energy levels of ^{84}Kr are shown in Fig. 2 and compared with experiments [1, 13]. It can be seen that the ordering of the calculated 0_2^+ , 2_2^+ and 4_1^+ levels in ^{84}Kr agrees with the observed ones. Besides these three levels known experimentally at an excitation energy of ~ 2 MeV, we also predict possible negative parity states of spin 4 and 5. Although the octupole vibrations are not included in the calculation, the energy of the 3_1^- state is also fairly well reproduced by the theory.

The components of the wave functions of the 0_1^+ , 0_2^+ , 2_1^+ , 2_2^+ , 2_3^+ , 2_4^+ , 3_1^+ , 4_1^+ , 4_2^+ , 1_1^+ levels in ^{84}Kr which

contributed more than 4% are listed in Table 2. It appears that the ground state has mainly a two-particle configuration, while the remaining states have mixed characteristics.

Experimental information on the multipole mixing ratios $\delta(E2/M1)$ are displayed in Table 3. We also show the theoretical results, which were obtained by associating with the experimentally observed states 2^\pm (2.759 MeV), 3^\pm (3.082 MeV) and 1^\pm (3.366 MeV), the calculated levels 2_4^+ (2.79 MeV), 3_1^+ (3.40 MeV) and 1_1^+ (3.49 MeV), respectively. By inspecting the experimental and theoretical results one sees that the measured ratios $\delta(E2/M1)$ for the cascades $2_2^+ \rightarrow 2_1^+ \rightarrow 0_1^+$ and $2_3^+ \rightarrow 2_1^+ \rightarrow 0_1^+$ are reproduced by the calculation. On the contrary, for the remaining four cascades the calculated results for the mixing ratios disagree with the experimental data not only in sign but also in magnitude. This fact may indicate that the measured levels at 2.759 MeV, 3.082 MeV and 3.366 MeV carry negative parity.

In ^{84}Kr nucleus the 2_1^+ state is a two-particle cluster of seniority zero coupled to one phonon, while the 2_2^+ state is a two-particle cluster of seniority two. The same situation may be found in other vibrational nuclei, as for example in Cd isotopes. This is a consequence of the fact that in these nuclei the lowest single-particle states are of higher spin and,

**Fig. 1.** Comparison of experimental levels of ^{83}Se (Ref. 12), ^{85}Kr (Ref. 10), ^{87}Sr (Ref. 9), ^{89}Zr (Ref. 12) and ^{91}Mo (Ref. 11) with the calculated spectra

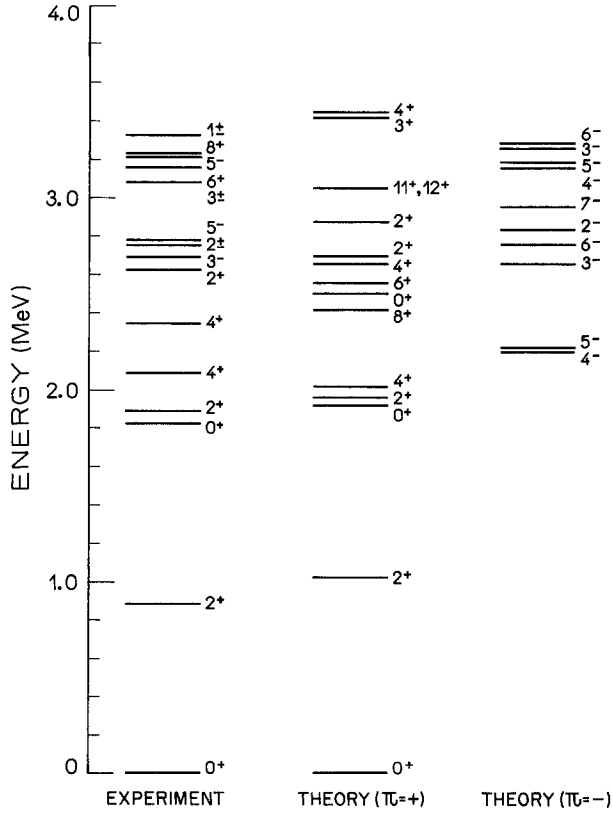


Fig. 2. Experimental [1, 13] and calculated level schemes for ^{84}Kr

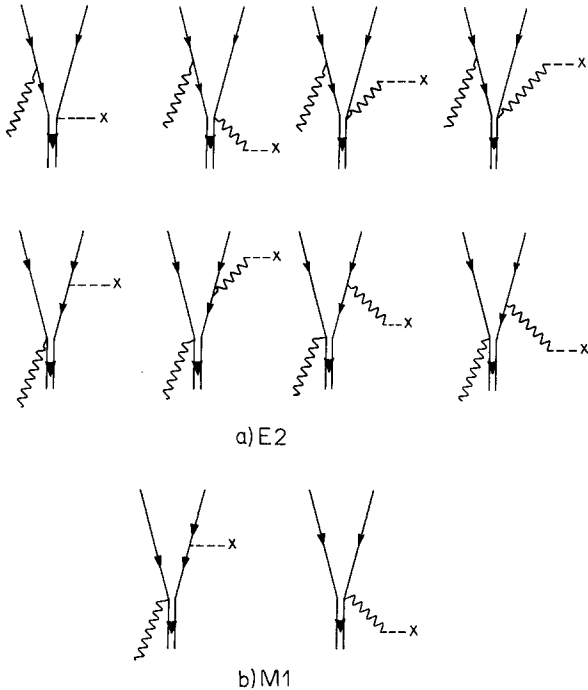


Fig. 3. Lowest order diagrams for the E2 (3a) and M1 (3b) transitions between the states 2_2^+ and 2_1^+ in ^{84}Kr

Table 2. Wave functions of a few low-lying states in ^{84}Kr . Only those amplitudes which are larger than 4% are listed

0_1^+		0_2^+	
$ (g_{9/2})^2 0,00\rangle$	0.76	$ (g_{9/2})^2 0,00\rangle$	0.33
$ (p_{1/2})^2 0,00\rangle$	-0.26	$ (p_{1/2})^2 0,00\rangle$	0.44
$ (p_{3/2})^2 0,00\rangle$	-0.24	$ (p_{1/2})^2 0,020\rangle$	0.23
$ (f_{5/2})^2 0,00\rangle$	-0.25	$ (g_{9/2})^2 2,12\rangle$	0.30
$ (g_{9/2})^2 2,12\rangle$	0.34	$ (p_{1/2}, p_{3/2}) 2,12\rangle$	-0.35
-	-	$ (p_{1/2}, p_{5/2}) 2,12\rangle$	-0.36
2_1^+		2_2^+	
$ (g_{9/2})^2 0,12\rangle$	0.66	$ (p_{1/2})^2 0,12\rangle$	-0.24
$ (p_{1/2})^2 0,12\rangle$	-0.25	$ (g_{9/2})^2 0,22\rangle$	0.38
$ (p_{3/2})^2 0,12\rangle$	-0.21	$ (g_{9/2})^2 2,00\rangle$	-0.43
$ (g_{9/2})^2 2,00\rangle$	0.37	$ (g_{9/2})^2 2,12\rangle$	0.35
$ (g_{9/2})^2 2,24\rangle$	0.22	$ (g_{9/2})^2 4,12\rangle$	-0.23
$ (f_{5/2})^2 0,12\rangle$	-0.22		
2_3^+		2_4^+	
$ (g_{9/2})^2 0,22\rangle$	-0.52	$ (p_{1/2}, f_{5/2}) 2,00\rangle$	-0.22
$ (p_{1/2})^2 0,22\rangle$	0.21	$ (p_{1/2}, p_{3/2}) 2,00\rangle$	-0.26
$ (g_{9/2})^2 2,00\rangle$	-0.50	$ (g_{9/2})^2 2,22\rangle$	0.20
$ (g_{9/2})^2 4,12\rangle$	-0.35	$ (g_{9/2})^2 0,12\rangle$	0.46
		$ (g_{9/2})^2 2,00\rangle$	-0.21
		$ (g_{9/2})^2 2,12\rangle$	0.31
		$ (g_{9/2})^2 2,24\rangle$	0.20
		$ (p_{1/2})^2 0,12\rangle$	0.22
		$ (g_{9/2})^2 0,22\rangle$	0.21
4_1^+		1_1^+	
$ (g_{9/2})^2 0,24\rangle$	0.43	$ (g_{9/2})^2 2,12\rangle$	0.78
$ (g_{9/2})^2 2,12\rangle$	0.47	$ (g_{9/2})^2 2,22\rangle$	-0.22
$ (g_{9/2})^2 4,00\rangle$	0.57	$ (g_{9/2})^2 4,24\rangle$	0.53
$ (g_{9/2})^2 6,12\rangle$	0.22		
3_1^+		4_2^+	
$ (g_{9/2})^2 0,33\rangle$	-0.27	$ (g_{p/2})^2 0,24\rangle$	0.47
$ (g_{9/2})^2 2,12\rangle$	0.64	$ (g_{1/2})^2 0,24\rangle$	-0.28
$ (g_{9/2})^2 2,22\rangle$	0.40	$ (p_{3/2})^2 0,24\rangle$	-0.21
$ (g_{9/2})^2 2,24\rangle$	-0.28	$ (g_{9/2})^2 4,00\rangle$	-0.56
$ (g_{9/2})^2 4,12\rangle$	0.29	$ (g_{9/2})^2 6,12\rangle$	-0.24
$ (g_{9/2})^2 4,22\rangle$	0.22	$ (f_{5/2})^2 0,24\rangle$	-0.21
$ (g_{9/2})^2 4,24\rangle$	0.20		

therefore, the pairing energy is large, depressing the multiplets below the broken pairs. Lowest order processes contributing to the $\langle I_i \| \mathcal{M}(E2) \| I_f \rangle$ and $\langle I_i \| \mathcal{M}(M1) \| I_f \rangle$ matrix elements are represented, respectively, by diagrams displayed in Fig. 3 a and 3 b. In the first case, for each single-particle diagram drawn on the left side correspond three induced collective diagrams drawn on the right-hand side, with all possible time-orderings of the emission or absorption of the virtual phonon. When the angular-momentum algebra is elaborated analytically the

Table 3. Comparison of the experimental and theoretical multipole mixing ratios. The calculated results for the last four cascades were obtained by assuming that the experimentally observed states 2^\pm (2.759 MeV), 3^\pm (3.082 MeV) and 1^\pm (3.366 MeV) correspond respectively to the theoretical levels 2_4^+ (2.79 MeV), 3_1^+ (3.40 MeV) and 1_1^+ (3.49 MeV)

Cascade	Multipole mixing ratio $\delta(E2/M1)$	
	Experimental	Theory
2_2^+ (1.898 MeV) \rightarrow 2_1^+ (0.882 MeV) \rightarrow 0_1^+	0.80 ± 0.03	0.75
2_3^+ (2.623 MeV) \rightarrow 2_1^+ (0.882 MeV) \rightarrow 0_1^+	-1.05 ± 0.07	-0.79
2^\pm (2.759 MeV) \rightarrow 2_1^+ (0.882 MeV) \rightarrow 0_1^+	-0.07 ± 0.03	0.32
3^\pm (3.082 MeV) \rightarrow 4_1^+ (2.095 MeV)		
\rightarrow 2_1^+ (0.882 MeV)	-0.08 ± 0.01	0.82
3^\pm (3.082 MeV) \rightarrow 4_1^+ (2.348 MeV)		
\rightarrow 2_1^+ (0.882 MeV)	-0.07 ± 0.01	0.17
1^\pm (3.366 MeV) \rightarrow 2_1^+ (0.882 MeV) \rightarrow 0_1^+	$+0.01 \pm 0.01$	-0.94

mixing ratio can be expressed in the form

$$\mathcal{D} = \frac{2}{3} \sqrt{\frac{5}{7}} \frac{(2j+5)(2j-3)}{2j(2j-1)} \frac{\Delta}{\hbar\omega} \frac{Q^{\text{sp}}(j)}{g_R - g_j^{\text{sp}}} e_{\text{eff}} \quad (9)$$

where the symbol j stands for the angular momentum of the dominant single particle-state ($j = g_{9/2}^{-1}$ for ^{84}Kr and ^{114}Cd), Δ is one-particle pairing energy and can be approximated as [14]

$$\Delta \approx \frac{12}{A^{1/2}} \text{ MeV}, \quad (10)$$

$Q^{\text{sp}}(j)$ and g_j^{sp} are, respectively, the single-particle quadrupole moment and the gyromagnetic ratio of the state j , and

$$e_{\text{eff}} = e_p^{\text{eff}} + \frac{5a}{4\sqrt{\pi}} \frac{\hbar\omega}{\Delta(\hbar\omega - \Delta)} e_v^{\text{eff}} \quad (11)$$

is an effective charge.

With the above mentioned parameters we obtain from (9) a value of $\mathcal{D} = 0.56$ while the exact result is $\mathcal{D} = 0.94$. In a similar calculation performed for the ^{114}Cd nucleus, with the usual parametrization [2], expression (9) yields a value $\mathcal{D} = -0.83$ which should be compared with the exact value $\mathcal{D} = -1.54$ and the experimental result [15] $\mathcal{D} = -2.2_{-0.3}^{+0.7}$. Therefore, we can conclude that the higher-order terms,

contributing to both the $E2$ and $M1$ transition moments and not included in the approximation (9) for the ratio \mathcal{D} , give rise to a change in magnitude but not in sign.

It is worth noting that recently Paar [16] has discussed, within the particle-vibration coupling model, the $E2/M1$ mixing ratios in odd-mass spherical and transitional nuclei. He obtained, for example, that for transitions of the type $\Delta N = 0$ between unique-parity yrast states

$$\mathcal{D}(j+2N \rightarrow j+2N-1) = \frac{\sqrt{5}}{2j} \left(\frac{2j+4N+2}{2j+4N-2} \right)^{1/2} \frac{Q^{\text{sp}}(j)}{g_j^{\text{sp}} - g_R} e'_{\text{eff}} \quad (12)$$

with

$$e'_{\text{eff}} = e_p^{\text{eff}} + \frac{5}{\sqrt{\pi}} \frac{a}{\hbar\omega} e_v^{\text{eff}}. \quad (13)$$

Therefore from (9) and (12) we can relate now the ratios of the odd-mass nuclei with those of the neighbouring even-mass nuclei.

IV. Conclusions

We have demonstrated that the property of the ^{84}Kr nucleus arises from neutron hole cluster with the quadrupole vibrational fields. Within this picture the experimentally energy spectrum and the mixing ratios $\delta(E2/M1)$ for the cascades $2_2^+ \rightarrow 2_1^+ \rightarrow 0_1^+$ and $2_3^+ \rightarrow 2_1^+ \rightarrow 0_1^+$ are well reproduced.

In addition, a simple rule for the sign and magnitude of the ratio \mathcal{D} is given for the vibrational nuclei in which the 2_1^+ and 2_2^+ states are, respectively, a two-particle cluster of seniority zero coupled to one phonon and a two-particle cluster of seniority two.

This work was supported by Fundação de Amparo à Pesquisa do Estado de São Paulo, and Conselho Nacional de Desenvolvimento Científico e Tecnológico.

References

1. Saxena, R.N., Jahnle, L.C., Zawislak, F.C.: Phys. Rev. C **21**, 1531 (1980)
2. Alaga, G.: In: Nuclear structure and nuclear reactions. Proceedings of the International School of Physics, "Enrico Fermi", Course XI. Jean, M., Ricci, R.A. (eds.). New York: Academic Press 1969
3. Paar, V.: In: Heavy-ion, high-spin states and nuclear structure. Vol. II, p. 179. Vienna: IAEA 1975
4. Krane, K.S., Steffen, R.M.: Phys. Rev. C **2**, 724 (1970)
Krane, K.S.: Phys. Rev. C **10**, 1197 (1974)

5. Kisslinger, L.S., Sorensen, R.A.: Rev. Mod. Phys. **35**, 853 (1963)
6. Cartwright, C.M., Forsyth, P.D., Holl, I., Irving, A.D., Martin, D.G.E.: J. Phys. G **7**, 65 (1981)
7. Blomquist, J., Wahlborn, S.: Ark. Fys. **16**, 545 (1960)
8. Boer, F.W.N. de, Fields, C.A., Samuelson, L.E.: Nucl. Phys. A **388**, 303 (1982)
9. Luksch, P., Tepel, J.W.: Nucl. Data Sheets **27**, 389 (1979)
10. Tepel, J.W.: Nucl. Data Sheets **30**, 181 (1980)
11. Muller, H.W.: Nucl. Data Sheets **31**, 181 (1980)
12. Lederer, C.M., Shirley, V.S.: Table of Isotopes. 7th Edn. New York: Wiley 1978
13. Muller, H.W., Tepel, J.W.: Nucl. Data Sheets **27**, 339 (1979)
14. Bohr, A., Mottelson, B.R.: Nuclear structure. Vol. I. New York: W.A. Benjamin, Inc. 1969
15. Lange, J., Kumar, K., Hamilton, J.H.: Rev. Mod. Phys. **54**, 119 (1982)
16. Paar, V.: Phys. Lett. **80 B**, 20 (1978)

H. Dias
Instituto de Física
Universidade de São Paulo
São Paulo
Brasil

F. Krmpotić
Departamento de Física
Facultad de Ciencias Exactas
Universidad Nacional de la Plata
C.C. 67
RA-1900 La Plata
Argentina

L. Losano
Departamento de Física
Universidade Federal de Paraíba
João Pessoa
Paraíba
Brasil

R.C. Mastroleo
Divisão de Física Teórica
Instituto de Estudos Avancados
Centro Técnico Aeroespacial
BR-12200 São José dos Campos, SP
Brasil